NewFields

Spatial Extent ("Footprint") and Volume of Macondo oil found on the deep-sea floor following the *Deepwater Horizon* oil spill

Scott A. Stout, Ph.D.[1], Shahrokh Rouhani, Ph.D.[2], Bo Liu, M.S.[1], Jacob Oehrig, M.S.[2]

[1]NewFields, Rockland, MA and [2]NewFields, Atlanta, GA
August 2015

ABSTRACT

The extent of Macondo oil from the *Deepwater Horizon* oil spill in benthic sediments was determined using a combination of chemical fingerprinting and a geostatistical interpolation method of kriging for 2397 sediments from 875 cores collected in 2010-2011 and 2014. The results show:

- The total mass of Macondo-derived hopane on the sea floor in 2010-2011 was conservatively estimated to be between 2.00 and 2.26 million grams. This mass is equivalent to 219,000 to 247,000 barrels of oil, which represents approximately 6.9 to 7.7 percent of the 3.19 million barrels released into the environment. The Macondo-derived hopane was deposited over at least 1,030 to 1,910 km^2 of sea floor.
- The total mass of Macondo-derived PAHs on the seafloor after the spill was conservatively estimated to be between 25.1 and 27.0 million grams, over an area of 1,440 to 2,280 km^2. Concentrations of $tPAH_{50}$ above 50,000, 20,000, 5000, and 1000 μg/kg covered approximately 2, 2, 42, and 412 km^2 of the seafloor, respectively. Concentrations of Macondo-derived $tPAH_{50}$ less than 1000 mg/kg covered between 983 and 1,820 km^2.
- Most (>97%) Macondo oil was found in surface (0-1 cm) and near-surface (1-3 cm) sediments, which is consistent with recent deposition of oil due to the extraordinary circumstance of the *Deepwater Horizon* oil spill – and inconsistent with long-term oil deposition from natural oil seeps.
- The 2010-2011 "footprint" of oil extends approximately 40 km to the southwest and less in other directions, indicating most seafloor oil was derived from fallout and/or scavenging (by marine snow) of oil from the deep-sea plume (which also extended southwesterly). Higher concentrations of Macondo oil found along the continental slope north and northwest of the well indicate direct impingement of the deep-sea plume also occurred ("bathtub ring").
- Although different approaches were used, our 2010-2011 results are comparable to those previously obtained by Valentine et al. (2014).
- Macondo oil is still present in surface sediments in 2014 although the total masses of hopane and $tPAH_{50}$ were significantly lower (~80 to 90%) compared to 2010-2011. We propose that these mass reductions are due to (1) biodegradation and/or (2) vertical mixing of the oil due to bioturbation since 2010-2011 may be responsible. Regardless, the significant reductions between 2010-2011 and 2014 re-affirms that the higher concentrations detected in 2010-2011

were unequivocally due to the "one-time" deposition of Macondo oil (and not long-term deposition from natural seeps).

INTRODUCTION

Crude oil released (April 20 to July 15, 2010) from the Macondo well at a water depth of 1500 m following the explosion of the *Deepwater Horizon* drill rig experienced different environmental fates. Buoyancy forces caused most of the oil to be transported (roughly) vertically ~1500 meters through the water column to the sea surface forming surface slicks, mousses, and sheens that were widely spread by wind and currents (Graettinger et al., 2015). However, some fraction of the released crude oil remained in the deep-sea.

Early sediment studies showed that some oil was directly deposited on the seafloor within 3 km of the well, aided in part by the oil's co-occurrence with dense synthetic based drilling mud (OSAT-1, 2010). Another fraction of the oil that had remained within the deep-sea was advectively transported horizontally as physically or chemically-dispersed, neutrally buoyant droplets (< 40 μm) within an extensive deep-sea "plume" that formed between ~1000 to 1300 m water depth (e.g., Camilli et al. 2010; Hazen et al., 2010; Socolofsky et al., 2011; Atlas 2011; Ryerson et al., 2012; Payne and Driskell, 2015). Deep water column studies tracked the plume in multiple directions, but mostly toward the southwest where oil droplets were still recognized 155 km from the well (dissolved chemical persisted much further; 267 km; Payne and Driskell, 2015).

Some of the oil that had reached the sea surface and some of the oil that remained within the deep-sea plume was ultimately deposited on the seafloor. Some surfaced oil sunk through its association with bacteria-mediated, mucus-rich marine snow that had proliferated in the near surface waters during the spill (Passow et al. 2012; Passow 2014). Direct evidence for this "marine oil snow" phenomenon was obtained in sediment trap samples collected during the active spill from a sediment trap located 58 km northeast of the well (VK826; Stout and German, 2015).

In addition, some of the oil that had remained within the deep-sea plume was also deposited on the seafloor. Some of this was likely "scavenged" and carried to the seafloor by bacteria-mediated, mucus rich marine snow particles that formed both at the surface and within the deep-sea plume. The sinking of marine oil snow from the sea surface and deep-sea plume to the seafloor led to the widespread accumulation of oil-bearing "floc" on the seafloor, a phenomenon that has been referred to as "*marine oil snow sedimentation and flocculent accumulation*" or MOSSFA (Kinner et al. 2014), the so-called "dirty blizzard" (Schrope, 2013).

Chemical evidence for the MOSSFA phenomenon and the widespread occurrence of seafloor floc containing Macondo oil was obtained from the study of deep-sea sediments (Valentine et al., 2014, Chanton et al., 2015; Brooks et al., 2015; Stout, 2015a), deep-sea corals (White et al., 2012; Hsing et al., 2013; Fisher et al., 2014; Brooks et al., 2015), and benthic infauna (Montagna et al., 2013). The collective results of these studies provide various means to assess the spatial extent, or "footprint", of the sunken Macondo oil (and floc) on the seafloor, although most of these studies were based upon observations made at only a few locations.

The Natural Resources Damage Assessment (NRDA) investigation led by the National Oceanic and Atmospheric Administration (NOAA), however, included the collection and chemical analysis of a large number (779) of sediment cores collected in late 2010 and 2011 during various NRDA cruises. These cores were subject to forensic investigation

in which the chemical concentrations of oil-derived hydrocarbons, spatial and depth trends, and chemical fingerprints were collectively used to determine which cores indicated the presence of Macondo oil (Stout, 2015a). An important component of the forensic study (Stout, 2015a) was a distinction between cores that contained oil-derived hydrocarbons derived from natural oil seeps within the deep sea – and not Macondo oil derived from the *Deepwater Horizon* oil spill.

In this study, we present our analysis of (1) the chemical concentration data collected for deep-sea sediment cores – *viz.*, 17α(H),21β(H)-hopane (hopane) and $tPAH_{50}$ – and (2) the forensic classifications by Stout (2015a) in quantifying the spatial extent ("footprint") of deep-sea sediments impacted by Macondo oil. We then calculate the collective mass of Macondo-derived hopane (i.e., non-seep and non-background hopane) within this "footprint" and, using hopane mass as a conservative tracer for the Macondo oil, calculate the mass (and corresponding volume) of Macondo oil deposited on the seafloor following the spill. Finally, using data from 201 cores collected in 2014, we conduct a comparable analysis to assess the spatial extent and mass/volume of Macondo oil still present on the seafloor four years after the oil spill.

Using the publically-available chemical concentration data from 2010-2011 (i.e., the same data we used), Valentine et al. (2014) conducted a similar assessment using hopane-concentration data only. These researchers used statistical means to establish "background" hopane concentration and did not distinguish Macondo- versus seep-derived hopane using chemical fingerprinting (as we have done). We compare our results to those of Valentine et al. (2014) and – given the slightly different approaches – find their study and ours to be highly comparable.

INVESTIGATED DATA AND ANALYTICAL METHODS

Investigated Data

Deep-sea sediment chemical concentration data were acquired from two web-based sources maintained by the NOAA, including:

> Data Integration Visualization Exploration and Reporting (DIVER), which is a collection of tools and processes to standardize and make available a vast range of data associated with the DWH spill (https://www.noaanrda.org/group/dwh/diver-explorer); and
>
> Environmental Response Management Application (ERMA®), which is an online mapping tool that integrates both static and real-time data, such as Environmental Sensitivity Index (ESI) maps, ship locations, weather, and ocean currents, in a centralized format (https://www.erma.noaa.gov/dwh/erma.html#/).

A total of 2211 samples from 691 unique sediment cores collected between July 22, 2010 and October 23, 2011 were used in our evaluation. 88 cores and 641 samples were excluded from our evaluation because they were determined to contain non-Macondo oil, i.e., naturally-seeped oil, sunken in situ burn residues, hydraulic fluid leaked from the remotely operated vehicle (ROV) during sediment coring, other unknown source of PAH or hopane not reasonably attributed to Macondo oil as determined during the forensic analysis (Stout, 2015a), and deeper depth (>10cm) sediments for which only limited number of samples existed. The 691 cores evaluated extended from approximately 110 miles southwest to 90 miles northeast of the Macondo wellhead. In addition, we used data from a total of 186 surface sediment (0-1 cm) samples collected

from 184 cores obtained during two 2014 NRDA surveys ("Irish Cruise 01 MAY 28 -JUN 11 2014" and "Irish Cruise 01 JUN 14 -JUN 28 2014"). 17 cores and 17 samples collected in 2014 were excluded from our analysis because they had been determined to contain naturally-seeped oil or other non-Macondo oil sources as stated earlier (Stout, 2015a). These cores extend from approximately 130 miles southwest to 134 miles northeast of the Macondo wellhead. (Although deeper intervals within the 2014 cores were analyzed, only the surface sediments were evaluated in our study.)

All of the 2010-2011 and 2014 sediment samples evaluated were collected from multiple NRDA work plans (Table 1). An inventory of the individual samples evaluated is provided in Attachment 1.

Sample Preparation and Analytical Methods

All sediments had been analyzed in accordance with (NOAA, 2014) by Alpha Laboratory (Mansfield, MA) via:

(1) Modified EPA Method 8015B to determine the TPH concentration (C_9-C_{44}) and concentrations of individual *n*-alkanes (C_9-C_{40}) and (C_{15}-C_{20}) acyclic isoprenoids via gas chromatography-flame ionization detection (GC/FID). Concentrations of target compounds were reported in $\mu g/kg_{dry}$.

(2) Modified EPA Method 8270 to determine the concentration of (a) approximately 80 PAH, alkylated PAH homologues, individual PAH isomers, and sulfur-containing aromatics and (b) approximately 50 tricyclic and pentacyclic triterpanes, regular and rearranged steranes, and triaromatic steroids via GC/MS operated in the selected ion monitoring mode (SIM). Concentrations of target compounds are reported in $\mu g/kg_{dry}$.

Our evaluation focuses on the concentration of 17α(H),21β(H)-hopane (hopane) and total PAH ($tPAH_{50}$) concentrations determined using the modified EPA Method 8270. $tPAH_{50}$ was calculated from 50 individual and co-eluted PAH compounds, as listed in Table 2, hereafter referred to as $tPAH_{50}$ (or in Figures, as simply TPAH). If the concentration of a given compound in a sample was below its reported detection limit, the compound concentration was treated as a 0 value in the summation of $tPAH_{50}$. Detection limits for samples described herein can be found in NOAA (2014), which were typically at or below 1 $\mu g/kg_{dry}$ for each PAH compound. Hopane and $tPAH_{50}$ concentrations (non-surrogated corrected) for the 2010-2011 and 2014 sediments are given in Attachment 1.

Forensic Analysis

As noted above, in order to quantitatively confirm the exposure of the deep-sea to Macondo oil, 3055 (2,852 in 2010-2011, and 203 in 2014) sediment samples were previously subjected to a forensic assessment (Stout, 2015a). This study resulted in the classification of each sediment sample into one of five classifications – "A" through "E" (Table 3). Sediments with an "A" or "B" classification contain Macondo oil. Sediments with a classification of "C" possibly had contained Macondo oil. Sediments with a "D" classification contained no oil, with any hydrocarbons present attributed only to "background". Finally, sediments with an "E" classification were considered to contain non-Macondo oil derived from naturally-occurring oil seeps within the deep-sea.

A summary of all forensic classifications for the 2010-2011 and 2014 results are shown in Attachment 1.

METHODOLOGY

In the present study, the extent of Macondo oil-impacted benthic sediments was determined by using the geostatistical interpolation method of *kriging*. This procedure produces the most accurate results based on well-defined statistical criteria. Kriging computes the weight of each measured value based on: (a) the computed spatial correlation of the dataset, often modeled by variograms; (b) the magnitude and direction of separation distances between measured points; (c) the magnitude and direction of separation distances between the interpolated location and its nearby measured points; and (d) the geometry of the measured and interpolated locations. Kriging also produces the measure of accuracy/reliability for each interpolated value, referred to as the prediction standard error (PSE). All geostatistical computations were performed using ArcGIS® Geostatistical Analyst software. The sediment data collected in 2010 and 2011 were treated as the first group data set, and the sediment data collected in 2014 were treated as the second group data set.

Computational Procedure

Determination and mapping of Macondo-derived hopane and $tPAH_{50}$ in deep-sea sediment samples collected between 2010 and 2011 were performed using the following procedural steps:

1. Compiled deep sediment hopane and $tPAH_{50}$ concentration data were divided into depth intervals as listed in Table 4. As noted above, any samples given a forensic classification of "E" (i.e., non-Macondo oil; Table 3) were excluded from further computations to prevent introduction of seep-derived hopane or PAHs into the datasets. In addition, several sediments determined to be impacted by sunken burn residues (Stout, 2015b) from the prolific *in situ* burning operations conducted during the response to the spill were excluded because these samples represented discrete, high concentration deposits of Macondo oil unrelated to the widespread deposition of oily floc from the MOSSFA event. Similarly, a few samples impacted by hydraulic fluid leaked from the ROV during sediment coring (and recognized via fingerprinting; Stout, 2015a) and a few samples with unknown source of PAH or hopane not reasonably attributed to Macondo oil as determined during the forensic analysis were excluded. These exclusions were aimed at avoiding any artificial increase in Macondo-derived hydrocarbon concentrations. Last, sediment samples from the deeper depth (>10cm) were excluded. In total, 641 samples were excluded (Attachment 1).
2. Hopane concentrations of all samples with "D" forensic classification (Table 3) were segregated and subjected to a thorough geostatistical analysis. Having contained no recognizable oil (Table 3), these samples were considered to contain only "background" or "ambient" hydrocarbons inherent throughout the deep-sea (but unassociated with any particular source). Upon determination of spatial correlations, kriging interpolation was used to compute depth-specific, ambient hopane concentrations over the entire sampled area, as depicted in

Figure 1. For this purpose, the sampled area was discretized into 1 km^2 grids, with estimation nodes at the center of each grid.

3. Interpolated ambient concentrations and their corresponding PSE were used to compute the ambient 95 percent upper confidence limit of the predicted (UCL) values at each estimation node. Depth-specific ambient values were then compared to their co-located measured sediment hopane concentrations associated with Match "A", "B" or "C" forensic results (Table 3). If the measured value was greater than the 95 percent UCL of the interpolated ambient hopane within the given grid, then the Macondo-related portion of hopane (i.e., "residual" or "excess" hopane) would be computed as the difference between the measured and interpolated ambient hopane concentration. If the measured value did not exceed the co-located 95 percent UCL of the interpolated ambient hopane concentration, it was assumed that the hopane concentration was statistically indistinguishable from ambient concentrations and the Macondo-related portion of hopane was set as zero. Similarly, all samples with "D" forensic results were assigned zero Macondo-derived hopane concentration.
4. The resulting Macondo-related residual hopane data were then subjected to a new round of geostatistical analysis and kriging. Each interpolated residual hopane concentration was applied to its corresponding 1 km^2 grid. These grid values represent the residual (excess) hopane concentrations attributable to Macondo oil, as shown in Figure 2.
5. The interpolated Macondo-impacted area was then subjected to further refinement in order to provide a conservative threshold for area and volume calculations.
    a. The first conservative exclusion was to remove any interpolated results "disconnected" from the main area of the Macondo impact (i.e. "islands"). After excluding these "islands" we considered the resulting areas as representing the *maximal* impacted area.
    b. The second conservative exclusion was to additionally remove (i) interpolated results with upper quartile PSE values, i.e., the least reliable estimates and (ii) interpolated results less than the lowest measured hopane residual. We considered the resulting areas as representing the *minimal* impacted areas.

    Figures 3 to 4 depict both the minimal and maximal impact areas and hopane concentrations for each depth interval.

The same analyses (Steps 1 through 5) were repeated for $tPAH_{50}$ results.

Total Mass and Volume of Macondo Oil in Deep-Sea Sediments

Depth-specific total mass and volume of Macondo oil in deep-sea sediments were calculated using the above cited residual hopane results (Figs. 3and 4). This approach assumes hopane in Macondo oil was not degraded in the samples studied, which is reasonable given its long-recognize recalcitrance to biodegradation (Prince et al., 1994). Total hopane mass was calculated as:

$$H_m = H_c * S_v * S_d \qquad \textit{Eq. (1)}$$

where

H_m = Hopane mass;
H_c = Interpolated Macondo-related (residual) hopane concentration;
S_v = Sediment volume which is calculated by multiplying depth-specific spatial extent of Macondo-related hopane concentration by its corresponding depth interval; and
S_d = Assumed floc-containing sediment density of 1.05 g/cm^3.

The latter (S_d) is obviously low for sediment consisting of siliciclastic minerals (~2.65 g/cm^3). We selected this low value because most surface sediment (0-1 cm) contained Macondo oil associated with the oily floc deposited during the MOSSFA event. This floc was easily disturbed and re-suspended due to its low density (J. Payne, personal communication). Therefore, as a conservative measure we used a density value close to water. This is a significant difference from the work of Valentine et al. (2014; see below).

The total mass of Macondo oil present in impacted sediments was calculated as the ratio of H_m to the average hopane concentration in fresh Macondo oil (68.8 μg/g$_{oil}$; Stout, 2015b). In turn, the total volume of Macondo oil was then determined using its measured density of 0.856 g/cm^3 at 5°C (Stout, 2015c).

Additionally, there were total of 203 surface sediment samples collected from two 2014 NRDA surveys (Table 1). The same computational procedures used for the 2010-2011 dataset (described above) were used in determining the Macondo-impacted area, total mass, and volume of Macondo oil based upon the 2014 surface sediments. The only modification employed in the 2014 calculations was to increase the major and minor semi-axis parameter during kriging interpolation of "ambient" (background) hopane and $tPAH_{50}$ concentrations, due to the smaller number of samples collected in 2014.

RESULTS AND DISCUSSION

Hopane Kriging – 2010-2011

Ambient Hopane: Figure 1 had shown the concentrations of ambient (background) hopane detected in surface sediments in which no "fingerprintable" oil was observed ("D" fingerprint classifications per Table 3). Figure 1A shows that the lowest concentrations of ambient hopane occur in shallower (<1000 m) sediment cores collected from the continental slope and shelf to the north and east of the Macondo well. Most surface sediments in this area contain less than 15 μg/kg of hopane. In deeper water (>1000 m) and within 50 km of the Macondo well, however, there are generally higher concentrations of ambient hopane with most sediments containing between 30 and 60 μg/kg, with some areas exceeding 90 μg/kg hopane (Fig. 1B). We attribute the higher ambient hopane concentrations in this area to a combination of long-term impacts from natural seeps in this area and the pervasive increase in hopane concentrations in surface sediments caused by the Macondo oil, even when it is not present in a sufficient concentration to recognize via chemical fingerprinting (i.e., too little oil to justify anything but a "D" fingerprint class; Table 3).

Macondo-derived Hopane: The 2010-2011 Macondo-derived (residual) hopane kriging interpolation results are summarized in Tables 5 and 6. These two tables reflect the

results obtained using the conservative steps described in Step 5 (above), the results of which we consider provide minimal (Table 5) and maximum (Table 6) estimates of the area impacted and corresponding range in the mass and volume of Macondo oil that was deposited on the seafloor.

Inspection reveals the Macondo oil was recognized to have covered between 1,030 to 1,910 km^2 of the seafloor surface (0-1 cm). Within these areas between 2.00 and 2.26 million grams of hopane was deposited in the top 10 cm of sediment, mostly in the surface (0-1 and 1-3 cm intervals; see below). In fact, more than 70% of the total Macondo oil was found in the top 0 to 1 cm and more than 97% of the total estimated Macondo oil deposited on the seafloor was found within the top 3 cm of sediments (Tables 5 and 6). By difference, of course, only 3% was predicted to be located within depth of 3 to 10 cm (all of this close to the well).

The fact that most (>70%) of the residual hopane in seafloor sediments was found in the upper cm of sediment (and >97% in the upper 3 cm) is consistent with its recent deposition of oil due to the extraordinary circumstance of the *Deepwater Horizon* oil spill in which a large volume of oil was (geologically-speaking) "instantly" added to the deep-sea. The lack of vertical mixing in the 2010-2011 cores points to a very recent source. The overwhelming presence of oil in the uppermost sediments only is inconsistent with a long-term input of oil such as might be attributed to the natural seeps in the area – and vertical mixing due to bioturbation. In fact, the input of oil from "long-lived" natural seeps is more likely represented by the "ambient" concentrations of hopane found in deeper sediments containing no obvious oil (i.e., fingerprint class "D"; Table 3).

The "footprints" and concentrations of Macondo-derived (residual) hopane in surface sediments (0-1 cm) and in the underlying sediment layer (1-3 cm) determined via kriging residual hopane concentrations are shown in Figures 3 and 4, respectively. As shown in Tables 5 and 6 these minimal and maximal footprints cover 1,030 to 1,910 km^2 of the seafloor surface. Inspection of either footprint reveals an overall northeast-to-southwest elongated spatial pattern that is distributed around the Macondo well. (The much smaller "footprints" associated with the 3-5 cm (100-539 km^2) and 5-10 cm (7-159 km^2) depth intervals are not shown, but these are also distributed around the Macondo well.) The fact that the footprints are distributed around the Macondo well is consistent with the well being the source of the hopane.

The "footprints" extend approximately 40 km to the southwest and less in other directions. The elongation of the footprints toward the southwest would be consistent with the predominant direction of the deep-sea plume, which preferentially carried particulate and dissolved phase oil in that direction (Camilli et al. 2010; Hazen et al., 2010; Socolofsky et al., 2011; Atlas 2011; Ryerson et al., 2012; Payne and Driskell, 2015). Elongation of the footprints in a southwesterly direction corroborates the contention that direct fallout from the deep-sea plume and/or "scavenging" of oil particles from the deep-sea plume by settling marine snow were the dominant mechanism(s) by which Macondo oil was spread within the deep-sea and carried to the deep seafloor. However, despite the predominant southwesterly direction, Macondo oil was also spread in all directions from the well indicating the deep-sea plume was not unvarying in its direction of transport (Figs. 3 and 4). Sediment trap studies on the shelf edge show that marine snow also carried oil from the sea surface to the seafloor (Stout and German, 2015), however, this mechanism of deposition appears secondary to oil derived from the deep-sea plume.

There are three features evident within the footprints that reveal additional detail regarding the mechanism of oil deposition. First, despite an overall decline with

increasing distance from the well there is some "patchiness" evident in hopane concentrations. We attribute this to the effects of sea floor topography and redistribution of the (apparently) low density oily floc by bottom currents, which may have caused preferential accumulation in localized bathymetric lows. Second, the concentration of Macondo-derived hopane is generally higher along an arc along the continental slope north and northwest of the well than in the area directly west of the well (Figs. 3-4). We attribute these slightly higher hopane concentrations along this arc to direct impingement of the deep-sea plume (~1000 to 1300 m) on the continental slope that rises in this area. Direct impingement of plume-entrained oil on the continental slope and other subsea features within the path of the deep-sea plume had been hypothesized, and referred to as a "*toxic bathtub ring*" (D. Hollander, 2011). The arc of higher Macondo-derived hopane concentrations would appear consistent with this mechanism of deposition (Fig. 3).

Finally, higher Macondo-derived hopane concentrations are observed approximately 20 km southwest of the well (Figs. 3-4). The cause for the higher concentrations observed in this area are uncertain, and largely due to data from an isolated core containing a high concentration of Macondo oil. It is possible, however, that some process(es) promoted oil particle deposition in this area. By analogy to a smokestack, it is conceivable that expelled particles fall at a preferred distance from the smokestack depending upon a combination of hydrodynamic factors. We hypothesize that there may have been some "smokestack-like" effect in which oil particles preferentially sunk from the deep-sea plume after traveling about 20 km within the plume. For example, it is possible that some combination of oil particle density (perhaps increased due to weathering during transport), plume velocity, or bathymetry promoted the deposition/accumulation of Macondo oil ~20 km southwest of the well.

Mass and Volume Estimates: The total mass of Macondo-derived hopane present within the minimal and maximal footprints corresponds to the deposition of 29.8 and 33.6 million kilograms of oil, which corresponds to the equivalent of 219,000 to 247,000 barrels of Macondo oil being deposited (and recognized as such) on the seafloor (Tables 5 and 6). The volume of Macondo oil discharged into the environment was determined to be 3.19 million barrels (Phase 2 Trial, U.S. District Court, 2015).

This means that we estimate between 6.9 and 7.7 percent of the oil discharged into the environment was deposited on the deep-sea floor. Because of our conservative assumptions, we consider this range to underestimate the total, especially considering that any Macondo-derived hopane that occurred within the nepheloid layer of suspended particles in cores (i.e., the supernatant of each core was poured off and analyzed separately from the sediment) is not included in this percentage. Regardless, this result makes it clear that the majority of the oil discharged did not end up on the deep-sea floor.

Hopane Kriging – Comparison to Previous Work

Valentine et al. (2014) used the 2010-2011 sediment core data to assess deposition of Macondo oil in the deep-sea and, like us, also used hopane as a conservative tracer. However, there are several differences between how these data were treated by Valentine et al. and in our study.

First, Valentine et al. did not include any chemical fingerprinting assessment of the source of hopane; specifically, any contribution of hopane by natural seeps to the excess hopane was included in their kriging of surface sediment residual hopane concentrations. This undoubtedly led to the overestimation of residual hopane in some

areas, e.g., northwest Biloxi Dome where numerous seeps were encountered in the sediment cores. These cores were excluded from our analysis (having been given an "E" fingerprint classification by Stout, 2015a; Table 3).

Second, Valentine et al. (2014) performed a numerical data analysis to distinguish "ambient" (background) hopane versus our use of chemical fingerprinting to recognize samples containing no obvious (fingerprintable) oil from any source (having been given and "D" fingerprint classification; Table 3). Numerical analyses performed by these researchers included studying the concentration difference between surficial and subsurface sediments of each given cores and the spatial distribution of hopane concentration as a function of the radial distance from the Macondo well, which established an ambient hopane concentration threshold for the entire area (28 ± 23 μg/kg). In our analysis of the data, in which chemical fingerprinting was utilized, we developed and used "site-specific" ambient hopane concentrations applied over 1 km^2 grids (e.g., see Step 2 in our Procedures, and Fig. 1).

Third, our analysis included Macondo-derived hopane within sub-surface sediments (>1 or 2 cm deep), whereas Valentine et al. (2014) considered only surface sediment (0-1 or 0-2 cm). Finally, we conservatively assumed that the density of the oily particles deposited was only 1.05 g/cm^3 while Valentine et al. assumed a much higher density of 2.65 g/cm^3. If we had selected a higher density we would have obtained (~2.5-times) higher hopane mass, and thereby higher total mass (and volume) of Macondo oil on the seafloor.

Despite these differences, the general features, sizes, and implications surrounding the oil deposition mechanisms the created the "footprints" determined by Valentine et al. (2014) and in our study are quite comparable. After several conservative assumptions (see Step 5 in our Procedures) we determined a Macondo-derived footprint covered 1,030 to 1,910 km^2 (Tables 5-6), whereas Valentine et al. (2014) estimated a footprint of approximately 3,200 km^2. However, because we limited our footprints to include only those cores in which the chemical fingerprint of any oil could still be confidently attributed to Macondo oil (per Stout, 2015a), our smaller footprints were conservative and thereby, expectedly smaller than if only excess hopane concentration was used. [Recall, if we use only $tPAH_{50}$ concentrations our footprints would be larger, 1,440 to 2,280 km^2 (Table 7), despite our conservative assumptions.]

Within their surface sediment footprint Valentine et al. (2014) calculated the presence of 1.8 ± 1.0 million grams of Macondo-derived hopane in surface sediments. Our more conservative approach yielded a marginally lower range, *viz.*, 1.43 to 1.62 million grams in surface sediments (Tables 5-6). If the additional mass of Macondo-derived hopane we determined exists in subsurface sediments (> 1 cm) is included, our total mass range increases to 2.0 to 2.26 million grams. Thus, in total, our two estimated masses of hopane that was deposited on the seafloor are highly comparable.

$tPAH_{50}$ Kriging – 2010-2011

The Macondo oil deposited on the seafloor, of course, contained PAHs, i.e., compounds directly associated with toxicity. Therefore, the concentrations of $tPAH_{50}$ in the 2010-2011 sediment data set were subjected to depth-specific geostatistical analysis and kriging. The results of this analysis are summarized in Table 7. Figures 5 and 6 show the corresponding $tPAH_{50}$ footprints for the 0-1 and 1-3 cm depth intervals.

In total, between 25.1 and 27.0 million grams of Macondo-derived $tPAH_{50}$ were detected on the seafloor in 2010-2011 (Table 7). As expected (as they parallel the hopane

results), more than 97% of total Macondo-derived PAHs were found in the top 3 cm of sediments (Table 7). As described above, this indicates the PAHs have a recent source.

Kriging determined that the Macondo-derived PAH covered an area estimated between 1,440 km^2 to 2,280 km^2 (Table 7; Figs. 5 and 6). These footprints are approximately 40% and 20% larger than the corresponding minimal and maximal hopane-predicted footprints (Tables 5 and 6, Figs. 3 and 4). These increases are mainly due to the fact that hopane is a single analyte whereas $tPAH_{50}$ represents the summed concentrations of up to 50 analytes. As such, about 3% of the seafloor sediment samples studied were shown to have a significant $tPAH_{50}$ residual but, owing to the absence of detectable hopane, did not exhibit any significant hopane residuals. Thus, the footprints of Macondo-derived hopane discussed in the previous section (Figs. 3 and 4) are additionally conservative when compared to the $tPAH_{50}$ footprints (Figs. 5 and 6).

The concentrations of Macondo-derived $tPAH_{50}$ in the seafloor sediments can be further investigated using the kriging results. Table 8 shows the "footprints" for surface (0-1 cm) and subsurface (1-3 cm) sediments containing different concentrations of Macondo-derived $tPAH_{50}$. This shows that ~2 km^2 of the seafloor surface sediments contained residual $tPAH_{50}$ concentrations above 50,000 μg/kg, which of course, were located proximal to the well (Fig. 5). On the other hand, between 983 and 1820 km^2 of the seafloor surface sediments contained residual $tPAH_{50}$ concentrations of less than 1000 μg/kg (Table 8).

The concentrations of $tPAH_{50}$ within the footprints exhibit comparable features to those discussed above regarding hopane concentrations. Specifically, $tPAH_{50}$ concentrations exhibit some "patchiness" but generally decreased with increasing distance from the well, which are features consistent with smaller-scale depositional heterogeneity emanating from a primary source. Like hopane, residual $tPAH_{50}$ concentrations were also somewhat elevated along the continental slope north of the well due to the "bathtub ring" effect noted above. Finally, elevated residual $tPAH_{50}$ concentrations were found in surface sediments about 20 km to the southwest perhaps attributed to fallout of oil particles from the deep sea plume akin to a downstream "smokestack" effect.

Spatial Extent ("Footprint") and Mass of Macondo Oil – 2014 Results

Hopane and $tPAH_{50}$ surface sediment data from the 2014 sediment core collection were subjected to depth-specific geostatistical analysis and kriging, as summarized in Table 9. (Recall, only results for the 2014 surface sediments, 0-1 cm, were analyzed in our study.)

The 2014 results indicate that between 0.26 and 0.28 million grams of Macondo-derived hopane, recognizable via chemical fingerprinting (Stout, 2015a), were still present in the deep sea surface sediments. This represents only about 17 to 18 percent of the total Macondo-derived hopane mass that was determined to be present in surface sediments in 2010-2011. Similarly, between 1.7 and 1.9 million grams of $tPAH_{50}$ were still recognized to be present in surface sediments in 2014 (Table 9). This represents only about 9 percent of the total Macondo-derived PAHs that were determined to be present in surface sediments in 2010-2011.

We contend the significant (~80 to 90%) reduction of masses of Macondo-derived hopane and PAH in surface sediments are caused by (1) biodegradation of the oil and/or (2) vertical mixing of the oil due to bioturbation since their original deposition. Our data cannot currently differentiate the relative impacts of these mechanisms. Regardless, however, the marked reductions in both hopane and $tPAH_{50}$ concentrations since 2010-2011 re-affirms that the higher concentrations detected in 2010-2011 were unequivocally

due to the "one-time" deposition of Macondo oil (and not from "long-lived" deposition of oil derived from natural seeps in the region).

The corresponding footprints of Macondo-derived hopane (482 to 568 km^2) and $tPAH_{50}$ (406 to 555 km^2) are correspondingly smaller too (Fig. 7). Although the spatial extent of impact is reduced since 2010-2011, the 2014 results still provide evidence for ongoing impact in the deep-sea sediments around the well and up to 30 km to its southwest.

References

Atlas, R. M. and T.C. Hazen, 2011. "Oil biodegradation and bioremediation: A tale of the two worst spills in U.S. history." *Environ. Sci. Technol.* 45: 6709-6715.

Brooks, G.R., Rebekka A. Larson, Patrick T. Schwing, Isabel Romero, Christopher Moore, Gert-Jan Reichart, Tom Jilbert, Jeff P. Chanton, David W. Hastings, Will A. Overholt, Kala P. Marks, Joel E. Kostka, Charles W. Holmes,and David Hollander, 2015. "Sedimentation pulse in the NE Gulf of Mexico following the 2010 DWH blowout". *PLoS ONE* **10(7)**: e0132341. doi:10.1371/journal/pone.0132341.

Camilli, R., C. M. Reddy, D. R. Yoerger, B. A. S. Van Mooy, M. V. Jakuba, J. C. Kinsey, C. P. McIntyre, S. P. Sylva and J. V. Maloney, 2010. "Tracking Hydrocarbon Plume Transport and Biodegradation at Deepwater Horizon." *Science* 330: 201-204.

Chanton, J., T. Zhao, B. E. Rosenheim, S. B. Joye, S. Bosman, C. Brunner, K. M. Yeager, A. Diercks and D. J. Hollander, 2015. "Using natural abundance of radiocarbon to trace the flux of petrocarbon to the seafloor following the Deepwater Horizon oil spill." *Environ. Sci. Technol.* 49: 847-854.

Fisher, C. R., P.-Y. Hsing, C. L. Kaiser, D. R. Yoerger, H. H. Roberts, W. W. Shedd, E. E. Cordes, T. M. Shank, S. P. Berlet, M. G. Saunders, E.A. Larcom, and J. M. Brooks, 2014. "Footprint of Deepwater Horizon blowout impact to deepwater coral communities". *Proc. Nat'l. Acad. Sci.* 111(32): 11744-11749.

Graettinger George, Jamie Holmes, Oscar Garcia-Pineda, Mark Hess, Chuanmin Hu, Ira Leifer, Ian MacDonald, Frank Muller-Karger, Jan Svejkovsky, Gregg Swayze, 2015. Integrating data from multiple satellite sensors to estimate daily oiling in the northern Gulf of Mexico during the *Deepwater Horizon* oil spill. Draft report to DARP, Jan. 9, 2015. (J. Holmes, Stratus Consutling, corresponding author).

Hazen, Terry C., Eric A. Dubinsky, Todd Z. DeSantis, Gary L. Andersen, Yvette M. Piceno, Navjeet Singh, Janet K. Jansson, Alexander Probst, Sharon E. Borglin, Julian L. Fortney, William T. Stringfellow, Markus Bill, Mark E. Conrad, Lauren M. Tom, Krystle L. Chavarria, Thana R. Alusi, Regina Lamendella, Dominique C. Joyner, Chelsea Spier, Jacob Baelum, Manfred Auer, Marcin L. Zemla, Romy Chakraborty, Eric L. Sonnenthal, Patrik D'haeseleer, Hoi-Ying N. Holman, Shariff Osman, Zhenmei Lu, Joy D. Van Nostrand, Ye Deng, Jizhong Zhou, and Olivia U. Mason, 2010. "Deep sea oil plume enriches indigenous oil degrading bacteria." *Science* 330: 204-208.

Hsing, P.-Y., B. Fu, ET AL. Larcom, S. P. Berlet, T. M. Shank, A. F. Govindarajan, A. J. Lukasiewicz, P. M. Dixon and C. R. Fisher, 2013. "Evidence of lasting impact of the Deepwater Horizon oil spill on a deep Gulf of Mexico coral community." *Elementa* 1(doi: 10.12952/journal.elementa.000012).

Matheron, G. Les Variables Régionalisées et Leur Estimation. Masson et Cie, Éditeurs. Paris. 1965.

Montagna, P. A., J. G. Baguley, C. Cooksy, I. Hartwell, L. J. Hyde, J. L. Hyland, R. D. Kalke, L. M. Kracker, M. Reuscher and A. C. E. Rhodes, 2013. "Deep-sea benthic footprint of the Deepwater Horizon blowout." *PLoS ONE* 8(8): e70540. doi:70510.71371/journal.pone.0070540.

NOAA, 2010a. Plan for Adaptive Water Column NOAA-NRDA Sampling (PAWNNS) Cruise Plan - HOS Davis 3, September 3, 2010 and Addendum.

NOAA, 2010b. Mississippi Canyon 252 Incident NRDA Tier 1 for Deepwater Communities: Work Plan and SOPs, June 27, 2010 and Addendum

NOAA,2010c. Reconnaissance Survey of Hard-Ground Megafuana Communities in the Vicinity of Deeowater Horizon Spill Site, October 19, 2010

NOAA, 2011a. Mississippi Canyon 252 Incident NRDA Sampling Plan Offshore and Deepwater Softbottom Sediment and Benthic Community Structure Survey, April 6, 2011

NOAA, 2011b. MC252 Deepwater Horizon Oil Spill Deep Benthis Communities and Water Column Data Collection March-April 2011 HOS Sweetwater ROV Sediment and Bottom-Water Sampling Cruise Plan, March 22, 2011

NOAA, 2011c. MC252 Deepwater Horizon Oil Spill Deep Benthis Communities and Water Column Data Collection July-September 2011 HOS Sweetwater ROV Sediment and Bottom-Water Sampling Cruise Plan, March 22, 2011 and Addendum

NOAA, 2011d. Deepwater Sediment Sampling to Assess Post-Spill Benthic Impacts from the Deepwater Horizon Oil Spill, May 20, 2011

NOAA, 2011e. Natural Hydrocarbon Seeps Study Plan, Final Draft, December 2, 2011

NOAA, 2012. NRDA Sampling Plan Mesophotic Reef Follow-Up Cruise Plan, August 1, 2012

NOAA, 2014. Analytical quality assurance plan, Mississippi Canyon 252 (Deepwater Horizon) natural resource damage assessment, Version 4.0. May 30, 2014.

NOAA, 2015. Deepwater Sediment Sampling to Assess Post-Spill Benthic Impacts from the Deepwater Horizon Oil Spill, June 19, 2015.

NOAA, BP-Cardno, Entrix, NRDA, 2010. NOAA/BP-Cardno ENTRIX NRDA Cooperative Deep Tow Cruise 2 December 2010 Arctic-HOS Davis 5-Sarah Bordelon Cruise Plan, Version X, December 2010

OSAT-1, 2010. Summary report for sub-sea and sub-surface oil and dispersant detection: Sampling and monitoring. Operational Science Advisory Team, Dec. 17, 2010.

Passow, U., 2014. "Formation of rapidly-sinking, oil-associated marine snow." *Deep-Sea Res.* Part II, Top. Stud. Oceanogr.: doi: 10.1016/j.dsr1012.2014.1010.1001.

Passow, U., K. Ziervogel, V. Asper and A. Diercks, 2012. "Marine snow formation in the aftermath of the Deepwater Horizon oil spill in the Gulf of Mexico." *Environ. Res.* Lett. 7: 11 p.

Payne, J.R. and W. Driskell, 2015. 2010 DWH offshore water column samples – Forensic assessments and oil exposures. PECI Report to the Trustees in support of the DARP, August, 2015.

Prince, R. C., D. L. Elmendorf, J. R. Lute, C. S. Hsu, C. E. Haith, J. D. Senius, G. J. Dechert, G. S. Douglas and E. L. Butler, 1994. "17α(H),21β(H)-hopane as a conserved internal marker for estimating the biodegradation of crude oil". *Environ. Sci. .Tech.* 28(1): 142-145.

Ryerson, Thomas B., Richard Camilli, John D. Kessler, Elizabeth B. Kujawinski, Christopher M. Reddy, David L. Valentine, Elliot Atlas, Donald R. Blake, Joost de Gouw, Simone Meinardi, David D. Parrish, Jeff Peischl, Jeffrey S. Seewald, and Carsten Warneke, 2012. "Chemical data quantify Deepwater Horizon hydrocarbon flow rate and environmental distribution." *Proc. Nat'l. Acad. Sci.* 109(50): 20246-20253.

Schrope, Mark, 2013. "Dirty blizzard buried Deepwater Horizon oil". *Nature*, doi:10.1038/nature.2013.12304

Socolofsky, S. A., E. E. Adams and C. R. Sherwood, 2011. "Formation dynamics of subsurface hydrocarbon intrusions following the *Deepwater Horizon* blowout". *Geophys. Res. Letters* **38**(L09602, doi:10.1029/2011GL047174): 6 p.

Stout, S.A., 2015. Chemical composition of fresh Macondo crude oil. NewFields Technical Report to DARP, August 2015.

Stout, S.A., 2015a. Chemical evidence for the presence and distribution of Macondo oil in deep-sea sediments following the Deepwater Horizon oil spill. NewFields technical report to the Trusteees in support of the DARP, August 2015.

Stout, S.A., 2015b. Chemical composition of floating Macondo oil during the Spring-Summer of 2010. NewFields technical report to the Trusteees in support of the DARP, August 2015.

Stout, S.A., 2015c. Physical Properties of Fresh and Weathered Macondo Crude Oil. NewFields technical report to the Trusteees in support of the DARP, August 2015.

Stout, S.A. and C. German, 2015. Characterization and flux of marine oil snow in the Viosca Knoll (Lophelia Reef) area due to the *Deepwater Horizon* oil spill. NewFields Technical Report to DARP, August 2015.

United States Environmental Protection Agency (EPA). "Basics of Pump-and-Treat Ground-Water Remediation Technology." EPA/600/8-90/003. March 1990b.

United States Environmental Protection Agency (EPA). "GEO-EAS (Geostatistical Environmental Assessment Software)." User's Guide. EPA/600/4-88/033. September 1988.

United States Environmental Protection Agency (EPA). "Geostatistics for Waste Management: A User's Manual for the GEOPACK (Version 1.0) Geostatistical Software System." EPA/600/8-90/004. January 1990a.

United States Environmental Protection Agency (EPA). "Guidance for Data Useability in Risk Assessment (Part A)." 9258.7-09A. April 1992.

United States Environmental Protection Agency (EPA). "Methods for Evaluating the Attainment of Cleanup Standards, Volume 1: Soils and Solid Media." EPA 230/02-89-042. February 1989.

Valentine, D. L., G. Burch Fisher, S. C. Bagby, R. K. Nelson, C. M. Reddy, S. P. Sylva and M. A. Woo, 2014. "Fallout plume of submerged oil from Deepwater Horizon." *Proc. Nat'l. Acad. Sci.* 10.1073/pnas.1414873111: 6 p.

White, Helen K., Pen-Yuan Hsing, Walter Cho, Timothy M. Shank, Erik E. Cordes, Andrea M. Quattrini, Robert K. Nelson, Richard Camilli, Amanda W. J. Demopoulos, Christopher R. German, James M. Brooks, Harry H. Roberts, William Shedd, Christopher M. Reddy, and Charles R. Fisher, 2012. "Impact of the Deepwater Horizon oil spill on a deep-water coral community in the Gulf of Mexico." *Proc. Nat'l. Acad. Sci.* 109(50): 20303-20308.

Table 1. List of NRDA work plans under which the deep-sea sediments evaluated herein were collected.

HOS Davis Water Chemistry September 2010 (NOAA 2010a)
Deep Benthic Camera Trap (NOAA 2011a)
NRDA Tier 1 for Deepwater Corals (NOAA 2010b)
Mesophotic Reef Plan (NOAA 2012)
Hardbottom Plan (NOAA 2010c)
NRDA Cooperative Deep Tow Cruise December 2010 (NOAA, BP-Cardno, Entrix, NRDA 2010)
HOS Sweetwater Sediment/Bottom Water Mar-Apr 2011 (NOAA 2011b)
HOS Sweetwater Sediment/Bottom Water Jul-Sep 2011 (NOAA 2011c)
Soft-Bottom Sediment Sampling Plan (NOAA 2011d)
Natural Hydrocarbon Seeps Plan (NOAA 2011e)
Soft-Bottom Sediment Sampling Plan (NOAA 2015)

Table 2. List of PAH Compounds summed to calculate $tPAH_{50}$ concentrations discussed herein.

Naphthalene	C3-Phenanthrenes/ Anthracenes	C3-Naphthobenzothiophenes
C1-Naphthalenes	C4-Phenanthrenes/ Anthracenes	C4-Naphthobenzothiophenes
C2-Naphthalenes	Dibenzothiophene	Benz[a]anthracene
C3-Naphthalenes	C1-Dibenzothiophenes	Chrysene/Triphenylene
C4-Naphthalenes	C2-Dibenzothiophenes	C1-Chrysenes
Biphenyl	C3-Dibenzothiophenes	C2-Chrysenes
Dibenzofuran	C4-Dibenzothiophenes	C3-Chrysenes
Acenaphthylene	Benzo(b)fluorene	C4-Chrysenes
Acenaphthene	Fluoranthene	Benzo[b]fluoranthene
Fluorene	Pyrene	Benzo[j]fluoranthene/ Benzo[k]fluoranthene
C1-Fluorenes	C1-Fluoranthenes/Pyrenes	Benzo[a]fluoranthene
C2-Fluorenes	C2-Fluoranthenes/Pyrenes	Benzo[e]pyrene
C3-Fluorenes	C3-Fluoranthenes/Pyrenes	Benzo[a]pyrene
Anthracene	C4-Fluoranthenes/Pyrenes	Indeno[1,2,3-cd]pyrene
Phenanthrene	Naphthobenzothiophenes	Dibenz[ah]anthracene/ Dibenz[ac]anthracene
C1-Phenanthrenes/ Anthracenes	C1-Naphthobenzothiophenes	Benzo[g,h,i]perylene
C2-Phenanthrenes/ Anthracenes	C2-Naphthobenzothiophenes	

Table 3: Forensic classification of deep-sea sediments employed by Stout (2015a).

Sample's Forensic Classification	Description	Practical Conclusion to NRDA
A	Chemical fingerprints and core characteristics are consistent with Macondo oil or differences can unequivocally be explained by external factors*; SBM is present near wellhead; co-occurs with slurp-gun filter or core supernatant classified as "A"	Macondo crude oil is present
B	Chemical fingerprints and core characteristics preclude unequivocal match but differences can be reasonably explained by external factors*; often lower concentrations than "A"	
C	Chemical fingerprints and core characteristics are equivocal but other lines of evidence** support the presence of Macondo oil; Concentrations often low	Macondo crude oil is possibly present
D	Chemical fingerprints and core characteristics are inconclusive and no other classification is justified; most often due to a very low hydrocarbon concentrations or (rarely) sediment contains hydrocarbons derived from hydraulic oil contamination	No oil is present, only “background”
E	Chemical fingerprints and core characteristics are inconsistent with Macondo oil and cannot be explained by external factors*	Macondo oil is absent; a different petroleum (seep) is present

*For example, weathering, mixing, low(er) concentrations, and/or interferences

**co-occurrence with or proximity to of A or B samples

Table 4. Sample Depth Intervals

Depth Layer	Definition
Surface	Upper depth=0
Subsurface1	Upper depth≥0, lower depth ≤ 3cm
Subsurface2	Upper depth≥0, 3 < lower depth ≤ 5cm
Subsurface3	Upper depth≥0, 5 < lower depth ≤ 10cm

Note: samples from deeper cores may be included in multiple depth layers (e.g., 0-10 cm will be used in the Surface, Subsurface1, Subsurface2, and Subsurface3 layers)

Table 5. Minimal estimate of Macondo oil impact area and Macondo-derived (residual) total hopane mass, total oil mass, and total oil volume deposited on the seafloor following the *Deepwater Horizon* oil spill. These more conservative totals, relative to Table 6, excluded unreliable predicted values, interpolated results less than the lowest measured hopane residuals, those disconnected from the main Macondo-impacted areas, as well as, any interpolated artifacts along the margins of the mapped areas; see Step 5b in Computational Procedures.

Hopane Kriging Estimate	area (km^2)	Hopane mass (g)	Macondo mass (kg)	Macondo volume (barrels)
Surface (0-1cm)	1,030	1,430,000	20,700,000	152,000
Subsurface 1 (1-3cm)	1,130	548,000	8,640,000	63,500
Subsurface 2 (3-5cm)	100	19,100	302,000	2,220
Subsurface 3 (5-10cm)	7	7,350	116,000	850
Total	na	2,000,000	29,800,000	219,000

Table 6. Maximal estimate of Macondo oil impact area and Macondo-derived (residual) total hopane mass, total oil mass, and total oil volume deposited on the seafloor following the *Deepwater Horizon* oil spill. Totals exclude interpolated values disconnected from the main Macondo-impacted areas; see Step 5a in Computational Procedures.

Hopane Kriging Estimate	area (km^2)	Hopane mass (g)	Macondo mass (kg)	Macondo volume (barrels)
Surface (0-1cm)	1,910	1,620,000	23,500,000	173,000
Subsurface 1 (1-3cm)	1,700	579,000	9,110,000	67,000
Subsurface 2 (3-5cm)	539	40,100	632,000	4,640
Subsurface 3 (5-10cm)	159	18,400	291,000	2,140
Total	na	2,260,000	33,600,000	247,000

Table 7. Estimate of impact area and Macondo-derived (residual) $tPAH_{50}$ mass deposited in the deep benthic sediments following the *Deepwater Horizon* oil spill.

	Minimal		Maximal	
$TPAH_{50}$ Kriging Estimate	area (km^2)	$TPAH_{50}$ mass (g)	area (km^2)	$TPAH_{50}$ mass (g)
Surface (0-1cm)	1,440	18,700,000	2,280	19,900,000
Subsurface 1 (1-3cm)	1,130	6,060,000	1,730	6,420,000
Subsurface 2 (3-5cm)	77	271,000	540	500,000
Subsurface 3 (5-10cm)	3	38,700	212	183,000
Total	na	25,100,000	na	27,000,000

Table 8. Minimal and maximal spatial extents ("footprints") in surface (0-1 cm) and sub-surface (1-3 cm) sediments containing Macondo-derived (residual) $tPAH_{50}$ in various concentration ranges. All areas given in km^2.

$tPAH_{50}$ Range (μg/kg)	Surface (min)	Surface (max)	Subsurface 1 (min)	Subsurface 1 (max)
> 50,000	2	2	0	0
$20{,}000 \leq tPAH_{50} < 50{,}000$	2	2	0	0
$5{,}000 \leq tPAH_{50} < 20{,}000$	42	42	4	4
$1{,}000 \leq tPAH_{50} < 5{,}000$	412	412	14	14
<1,000	983	1,820	1,120	1,720
Total area (km^2)	1,440	2,280	1,130	1,730

Table 9. Estimate of surface residual of impact area, total hopane and $tPAH_{50}$ mass, Macondo oil mass and total spilled oil volume in the 2014 deep benthic sediments.

Surface Sediment	Hopane Kriging Estimate				$tPAH_{50}$ Kriging Estimate	
	area (km^2)	Hopane mass (g)	Macondo Oil mass (kg)	Macondo Oil volume (bbl)	area (km2)	$TPAH_{50}$ mass (g)
Minimal	482	258,000	3,750,000	27,500	406	1,670,000
Maximal	568	280,000	4,070,000	29,900	555	1,870,000

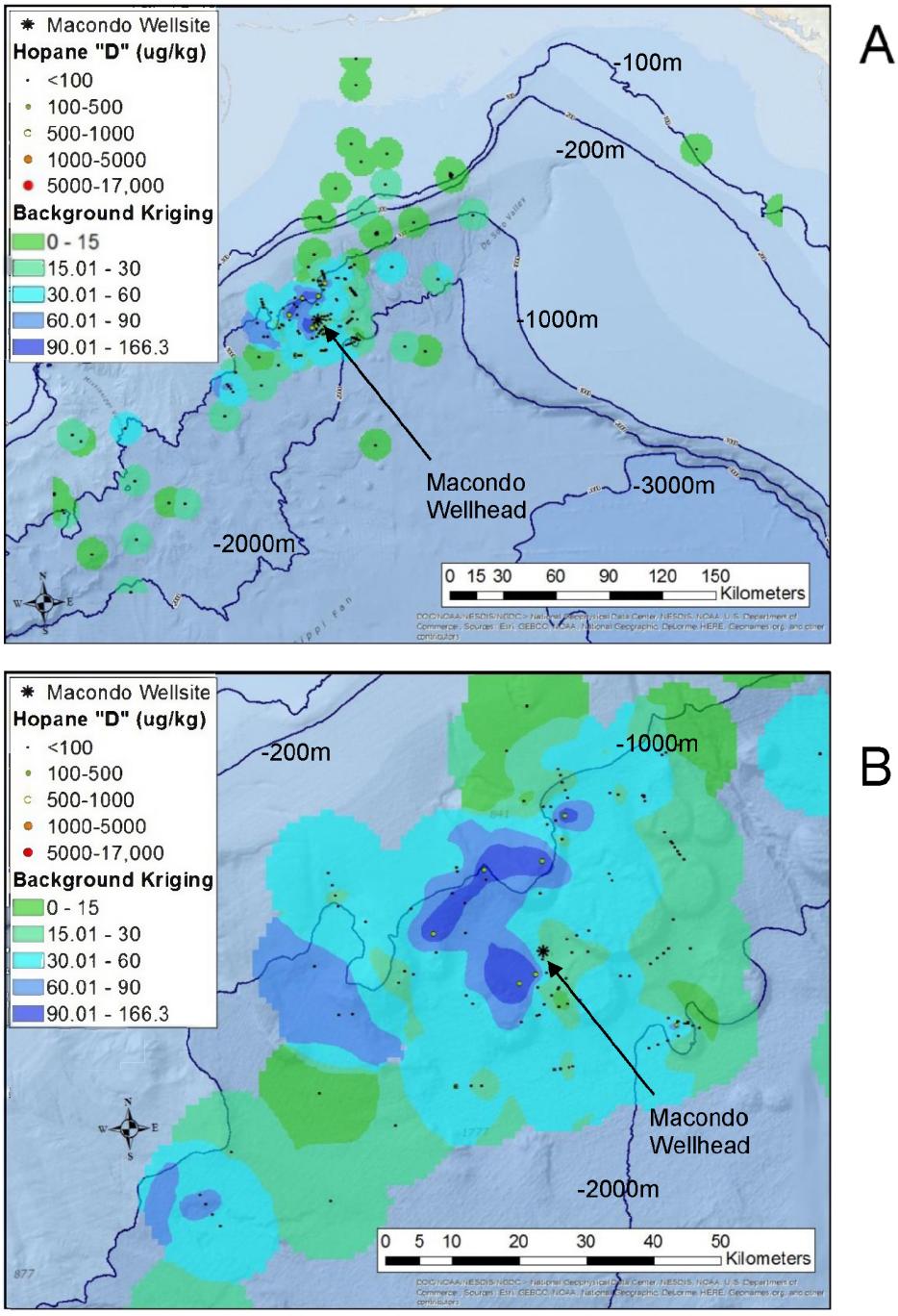

Figure 1. Kriging interpolated results for ambient (background) hopane values within surface (0-1 cm) soft bottom sediments collected in 2010-2011. (A) larger scale; (B) area closer to wellhead.

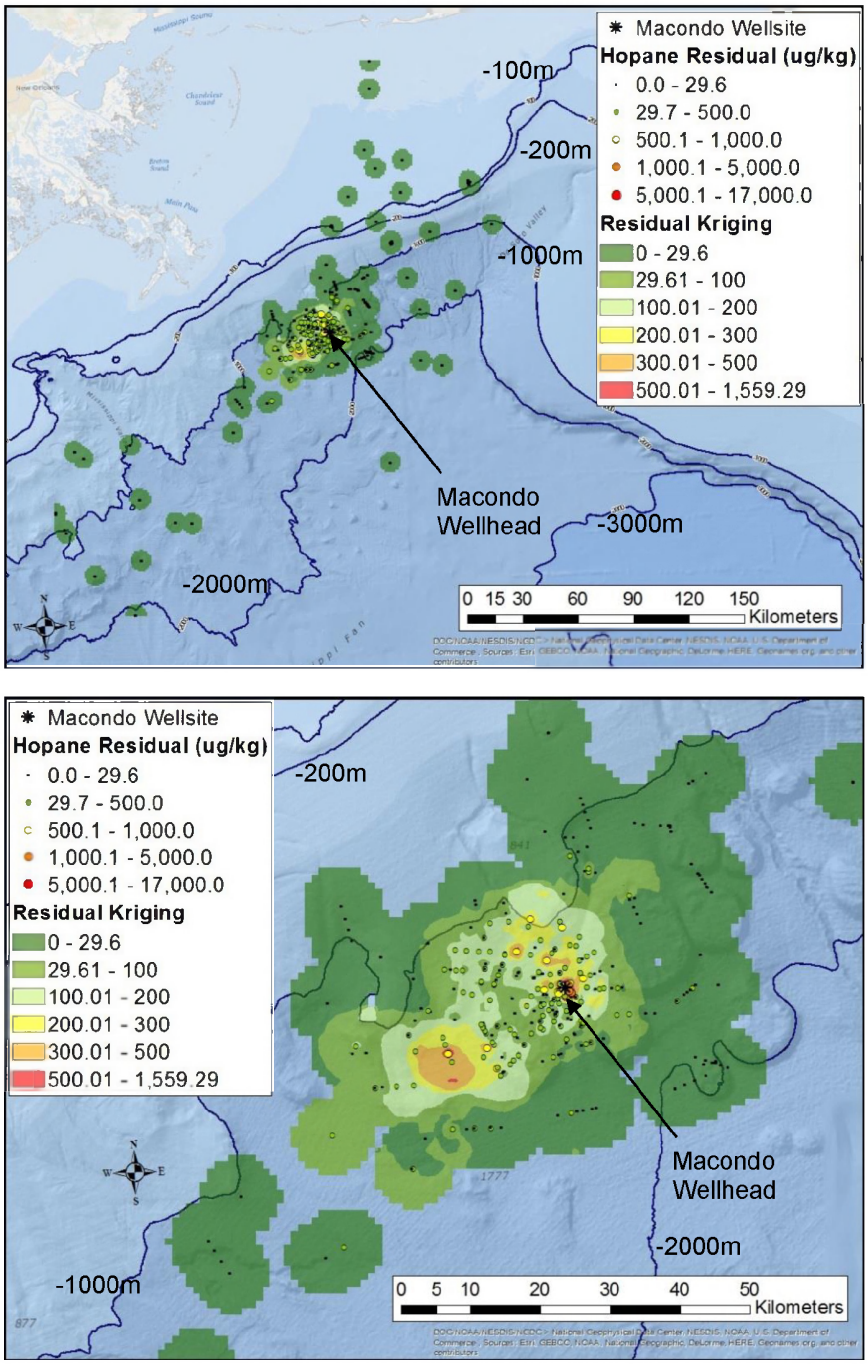

Figure 2. Macondo-related hopane residual kriging results for surface (0-1 cm) soft bottom sediments collected in 2010-2011. (A) larger scale; (B) area closer to wellhead.

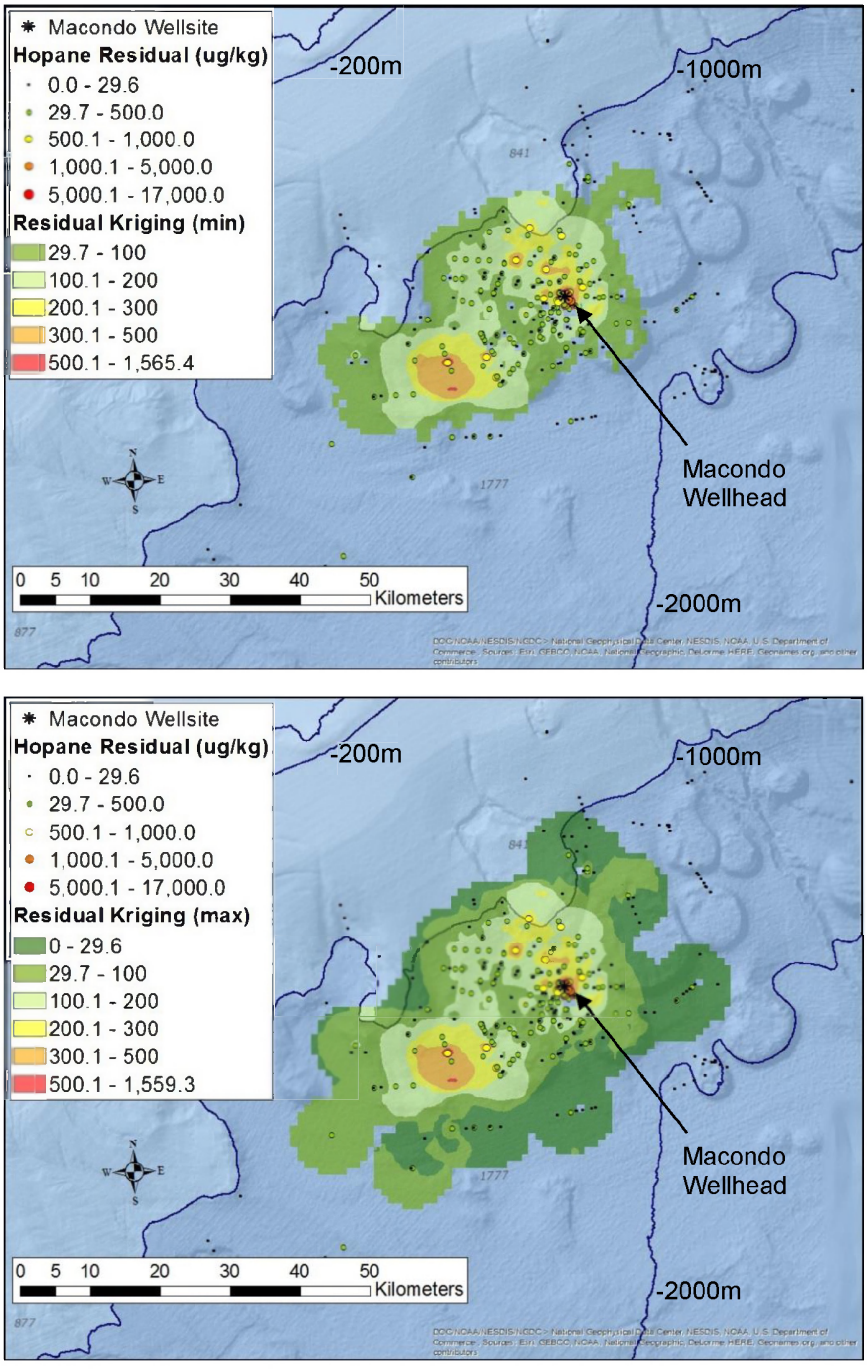

Figure 3. Macondo-derived hopane residual "footprints" determined from the kriging results for the 0 to 1 cm depth interval of deep-sea sediments collected in 2010-2011. (A) Minimal (1030 km^2) and (B) Maximal (1910 km^2). Grid blocks = 1 km^2.

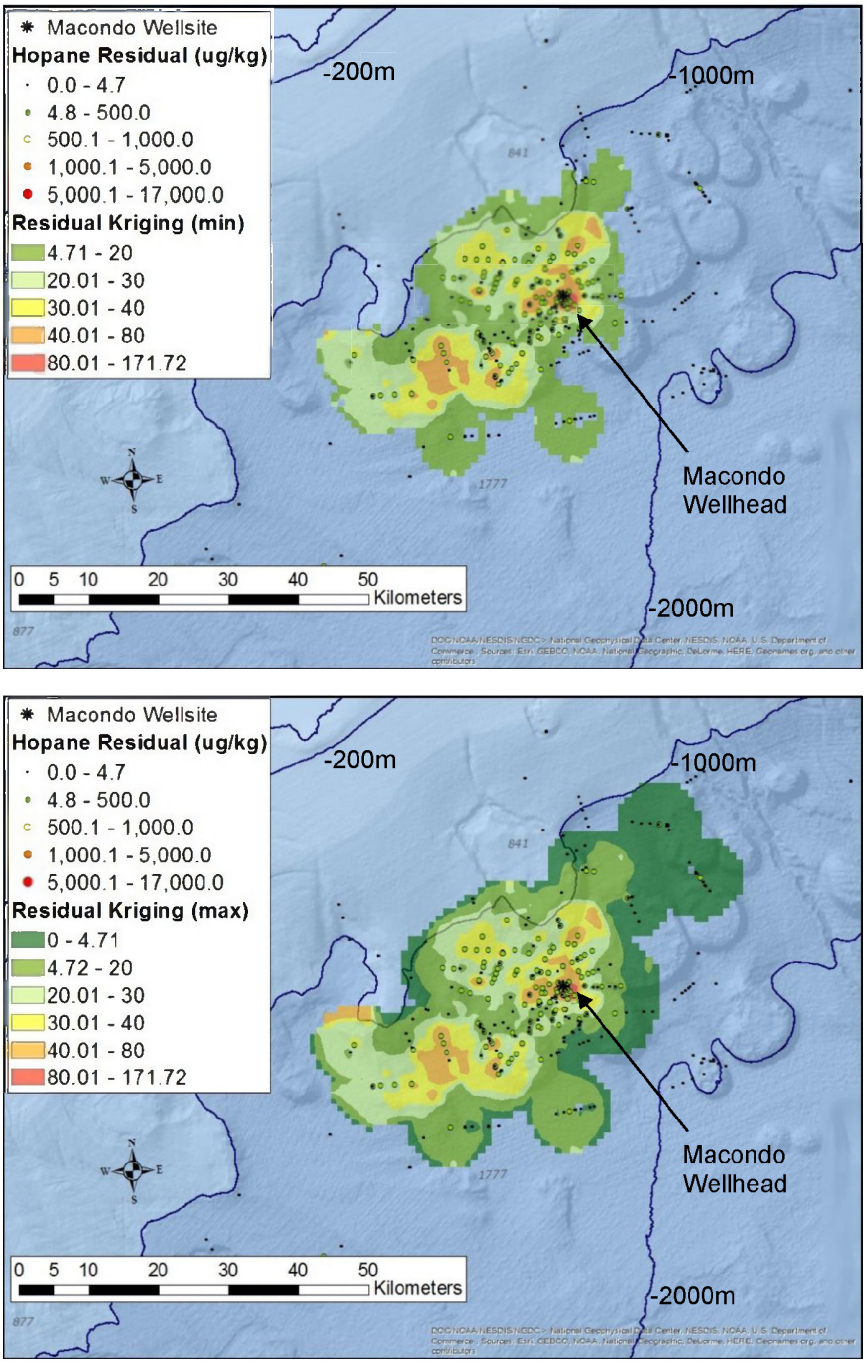

Figure 4. Macondo-derived hopane residual "footprints" determined from the kriging results for the 1 to 3 cm depth interval of deep-sea sediments collected in 2010-2011. (A) Minimal (1130 km^2) and (B) Maximal (1700 km^2). Note the colors corresponding to hopane residual concentrations in the 1-3 cm sediments (above) are much lower than in 0-1 cm sediment (Fig. 3).

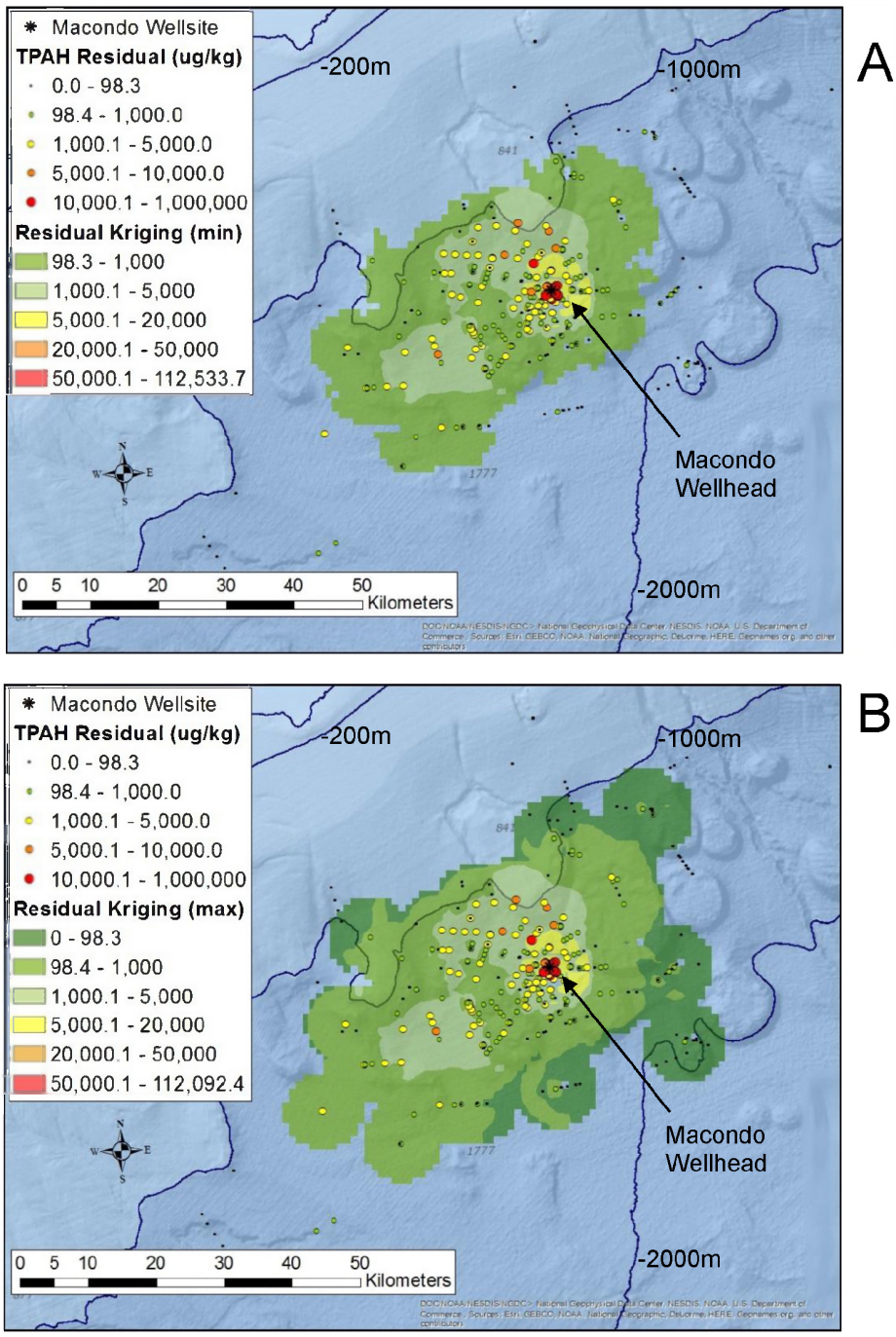

Figure 5. Macondo-derived $tPAH_{50}$ residual kriging results for surface (0-1 cm) sediments collected in 2010-2011. (A) Minimal (1440 km^2) and (B) Maximal (2280 km^2).

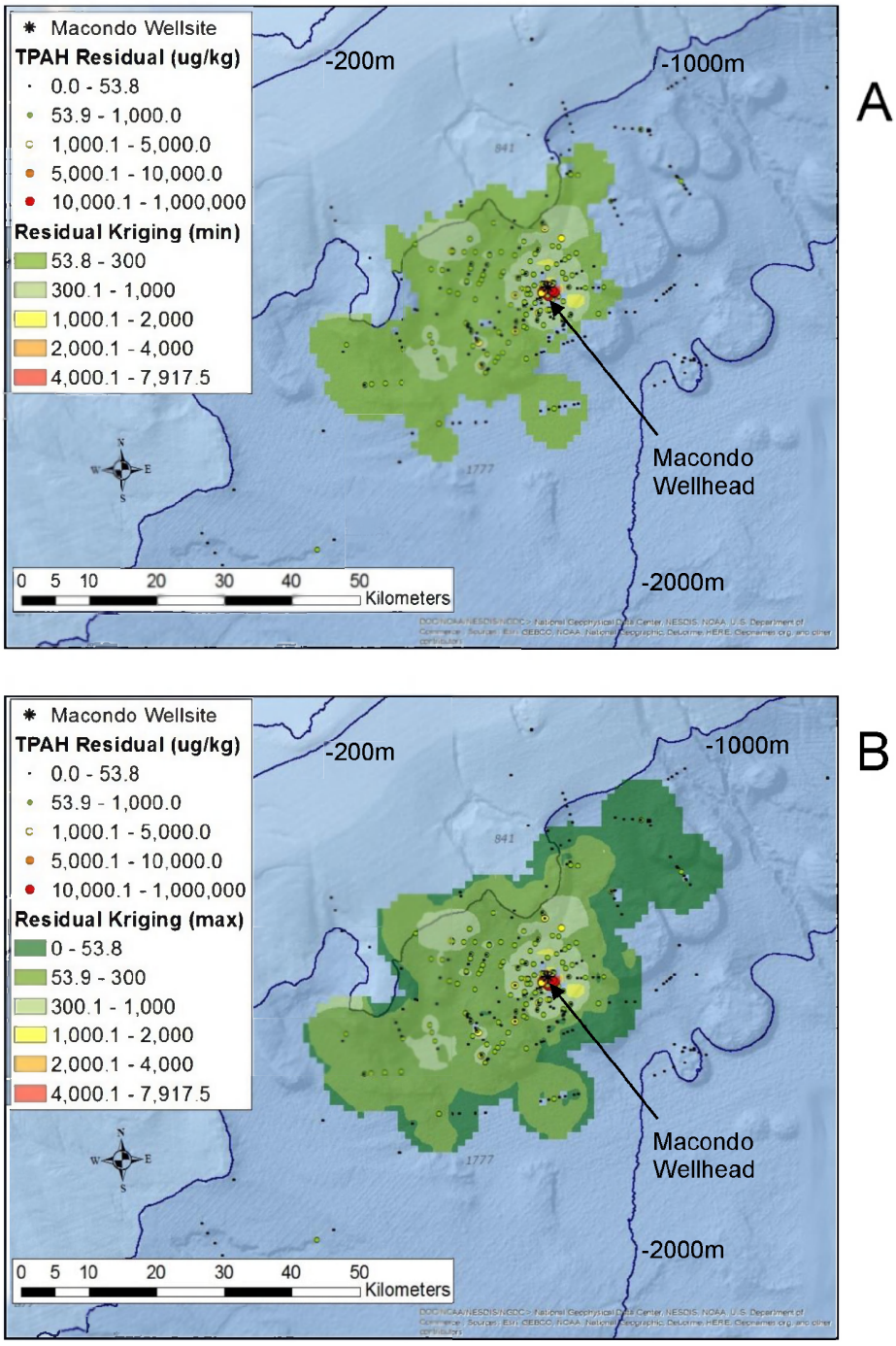

Figure 6. Macondo-related $tPAH_{50}$ residual kriging results for subsurface (1-3 cm) sediments collected in 2010-2011. (A) Minimal (1130 km^2) and (B) Maximal (1730 km^2).

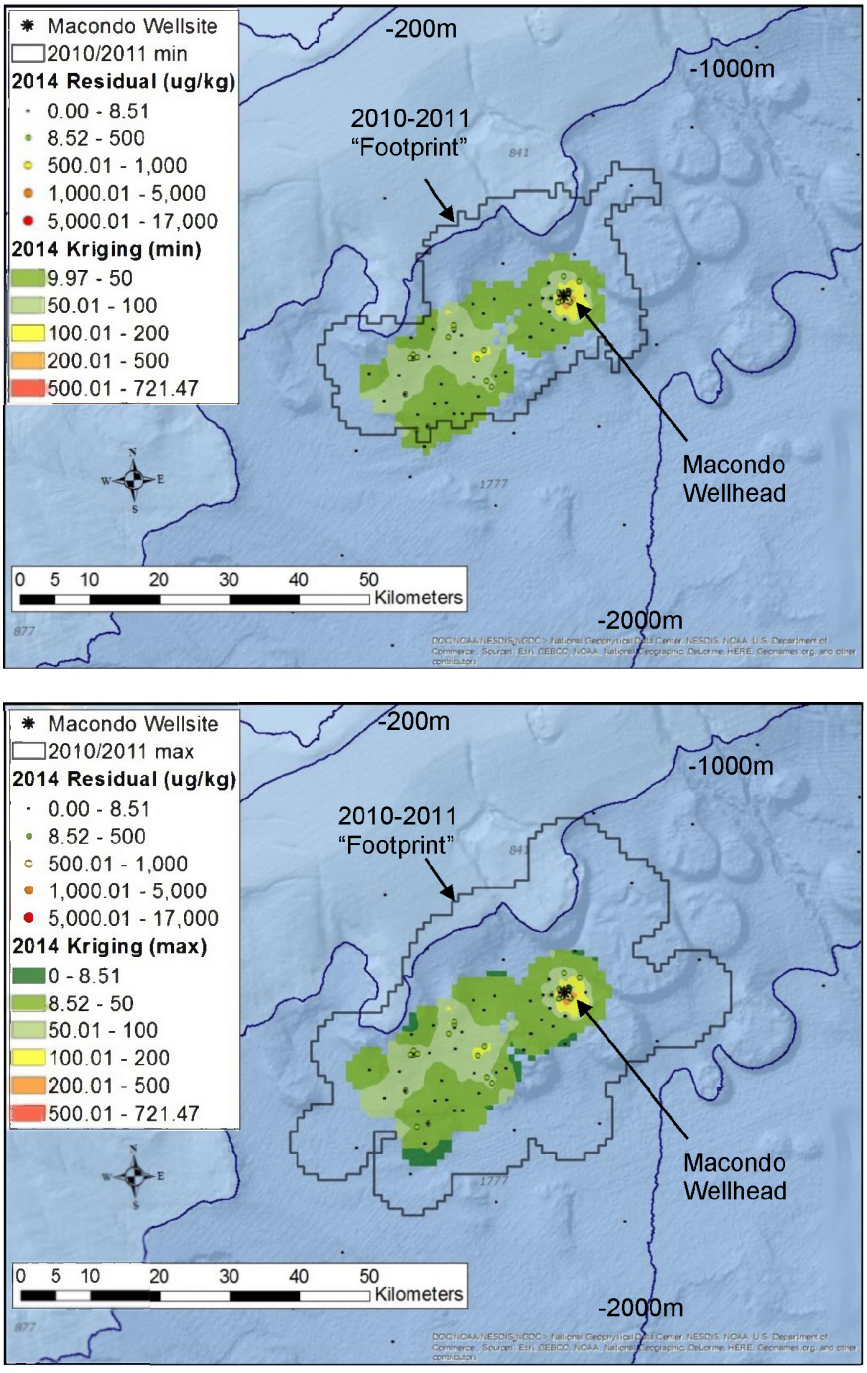

Figure 7. Macondo-derived hopane residual "footprints" determined from the kriging results for the 0 to 1 cm depth interval of deep-sea sediments collected in 2014. (A) Minimal (482 km^2) and (B) Maximal (568 km^2). Also depicted are the minimal and maximal "footprints" determined in 2010-2011 (from Fig. 3).